UNIVERSITA' DEGLI STUDI DI PARMA

Dottorato di ricerca in BIOLOGIA E PATOLOGIA MOLECOLARE

Ciclo XXVII

Novel approaches to corneal angiogenesis: macrophages, angiopoietin and VEGFs

Coordinatore:
Chiar.ma Prof.ssa Valeria Dall'Asta

Tutor:
Chiar.mo Prof. Pier Giorgio Petronini

Dottorando: Giulio Ferrari

Novel approaches to corneal angiogenesis: macrophages, angiopoietin and VEGFs

INTRODUCTION

The cornea is the outermost layer covering the eye anteriorly. It is constituted of three layers: epithelium, stroma and endothelium. The cornea receives nutrients from the aqueous humor, which bathes the corneal inner surface (i.e. endothelium) and by the tear film, which covers the outer surface (i.e. the epithelium). The normal cornea receives no vascular supply, as blood and lymphatic vessels arrest abruptly at the cornea periphery, in an area known as limbus. This allows the cornea to be perfectly transparent, which is essential for proper vision. Ingrowth of neovessels follows severe ocular ailments such as injuries, infections or autoimmune diseases. The development of neovessels reduces corneal transparency in two ways. First, blood is opaque, and blocks light. Second, the neovessels are not completely functional, because they lack pericytes and the basal membrane, hence they leak lipids, calcium and protein, which are deposited in the surrounding tissues and

induce opacification and inflammation. Corneal neovascularization represents a relevant clinical challenge. While cataract is responsible for approximately 20 million over the 45 million people who are blind worldwide, the next more prevalent cause is trachoma, which affects nearly 5 millions. Trachoma, a parasitic disorder affecting the eyelids, conjunctiva and the cornea, induces blindness through scarring and development of corneal neovascularization. Additionally, it is estimated that ocular trauma and infections, which are generally associated with corneal neovascularization, may be responsible for up to 2 millions of new cases of monocular blindness every year.

Childhood blindness affects approximately 1.5 million children worldwide. Among its causes, a relevant role is played by disorders associated with corneal neovascularizazion, such as xerophthalmia, commonly associated with vitamin A deficiency, ophthalmia neonatorum, and, more rarely, with herpes or vernal keratoconjunctivitis (Whitcher et al, 2001).

Indeed, corneal neovascularization (CNV) is the second most common cause of blindness worldwide (Skobe & Dana, 2009); its incidence in the US being 1.4 million per year (Azar, 2006). Typically, corneal neovessels develop in case of damages to the corneal stroma (Chang et al, 2001), while more superficial (i.e. epithelial only) injuries rarely result in robust vessel growth. The etiopathology of corneal neovascularization varies depending on a

geographical basis. More specifically, in the western countries and the US herpes keratitis represents the most common cause, while in developing countries, as in Africa, infectious keratitis, including trachoma, are the most prevalent.

Herpes simplex is the most common cause of infectious keratitis; it mainly affects the corneal stroma and it has been proposed that the development of corneal neovessels is instrumental to the development of the keratitis. Finally, a number of bacterial keratitis can result in corneal neovascularization. Bacteria involved include Streptococcus, Staphylococcus, and Pseudomonas species.

Treatments for corneal neovascularization can be either medical or surgical. Among medical treatments, topical use of corticosteroid eye drops has been the mainstay of therapy for a long time. This treatment, however, is variably effective and needs to be prolonged in time. Additionally, it is associated with a number of side effects, such as delayed wound healing, induction of cataract, increased intraocular pressure and even increased susceptibility to infections (Akpek et al, 2004). For these reasons, novel treatments have been attempted. Recently, anti-VEGF drugs have been proposed to treat corneal neovascularization. Their use, however, has been associated with corneal perforations, and delayed nerve regeneration. Moreover, while they seem

effective in blocking recent corneal neovascularization, their activity on stable corneal neovascularization is still under scrutiny.

With regards to surgical treatments, closure of neovessels has been attempted with bipolar electrodes, argon laser, or photodynamic therapy (Gerten, 2008; Pillai et al, 2000;Sugisaki et al, 2008). Electrocoagulation seems effective in the majority of cases, although there is the risk of inducing intracorneal hemorrhages, and long term results are still missing.

Apart from being a relevant ocular disorder, corneal neovascularization has a long history as a solid testing ground for anti-angiogenic treatments in oncology and other fields (Cao et al, 2011; Gimbrone et al, 1974).

Several anti-angiogenic factors have been isolated in the corneal epithelium. These include soluble Vascular Endothelial Growth Receptor 1 (sVEGFR-1) (Ambati et al, 2006), ectopic VEGFR-3 (Cursiefen et al, 2006; Singh et al, 2013), and others (Albuquerque et al, 2009; Sekiyama et al, 2006).

Indeed, the cornea is a well known immune privileged site. It is also known that the immune privilege is strongly associated with the angiogenic privilege. In this vein, it has been demonstrated that growth of corneal neovessels induces loss of the immune privilege, while the inhibition of vessel growth may restore immune privilege. The fact that corneal lymphangiogenesis is not clinically or histologically clearly visible caused

this field to be neglected for many years. It was only at the end of the last century, with the discovery of novel lymphatic markers, such as LYVE1 and Podoplanin, made it possible to study corneal lymphangiogenesis. Similarly, novel animal models allowed to segregate corneal angiogenesis from corneal lymphangiogenesis (Chang et al, 2002). In the clinical setting, corneal transplantation, also known as keratoplasty, is a procedure commonly performed to restore corneal transparency when it is lost. It has been shown that, post-keratoplasty, development of CNV occurs in one out of two cases (Cursiefen and Kruse, 2006). Interestingly, it has been suggested that lymphangiogenesis may be even more detrimental for the interruption of the corneal immune privilege. Indeed, it is through lymphatic vessels that immune cells gain access to lymph nodes and can start immune rejection (Chung et al, 2009).

Following pro-inflammatory insults to the cornea, an "angiogenic switch" (Hanahan & Folkman, 1996) occurs and CNV develops. Although generally associated with vision reduction, which may jeopardize survival in higher animals, the growth of neovessels is also beneficial as it helps recruiting and activating cellular immunity and provides protection against ocular perforation in corneal infections (Titiyal et al, 2006). Hence, avascularity of the cornea, constantly exposed to the outer environment, is considered the result of an evolutionary compromise between a prompt and

effective reaction to aggression from the outside and the avoidance of corneal opacification.

Tissue-recruited bone marrow-derived cells, such as macrophages, produce angiogenic factors and therefore may represent relevant players in corneal angiogenesis (Nucera et al, 2011). In fact, systemic depletion of macrophages suppresses CNV (Cursiefen et al, 2004). We previously described the role of TIE2-expressing monocytes (TEMs) in tumor neo-angiogenesis. These cells express the Angiopoietin receptor TIE2, which is upregulated upon homing to tumors and differentiation into perivascular macrophages (De Palma et al, 2008; De Palma et al, 2005; De Palma et al, 2003). These TIE2-expressing macrophages have features of M2 tumor-associated macrophages (TAMs) (Mantovani & Sica, 2010), promote both developmental and tumor angiogenesis (Fantin et al, 2010; Pucci et al, 2009), and are required for the formation of tumor blood vessels (De Palma et al, 2005; De Palma et al, 2003).

The Angiopoietins (ANG1–ANG4) and their TIE receptors (TIE1 and TIE2) play an essential role in vascular remodeling and vessel integrity (Saharinen et al, 2011). ANG2 can act as a partial agonist or an antagonist of TIE2, and has a destabilizing effect on the vasculature, resulting in either vascular growth or regression. Specifically, the release of ANG2 promotes angiogenesis by sensitizing endothelial cells to proliferation signals mediated

by other proangiogenic factors, namely VEGF (Augustin et al, 2009; Saharinen et al, 2010). In addition, ANG2 induces the expression of pro-angiogenic factors in TEMs (Coffelt et al, 2010). In the absence of pro-angiogenic factors, however, ANG2 promotes vessel regression. Blockade of ANG2 impedes upregulation of TIE2 in TEMs, and their ability to promote angiogenesis in tumors (Mazzieri et al, 2011).

Similarly to tumors, also in the cornea the growth of new vessels is frequently associated with infiltration of inflammatory cells, such as macrophages (Ogawa et al, 1999). The exact role of TEMs and ANG2 in CNV, however, has not been investigated yet.

Here, we report for the first time in mice *and* humans that: (i) ANG2 is expressed by the normal corneal epithelium and rapidly released upon injury; (ii) ANG2 release is related with injury severity; and (iii) TEMs are elective residents of the *normal* cornea and play an essential role in promoting CNV in response to ANG2.

These findings identify TEMs and ANG2 as important players modulating the angiogenic privilege of the normal cornea and can have relevant clinical implications.

AIM OF THE STUDY

The aim of this study is to test whether macrophages, and, more specifically, the macrophage sub-population expressing the Tie2 receptor (TEMs), are involved in the development of corneal neovessels. In addition, I will test whether the inhibition of TEMs is able to induce vessel regression. This will be achieved through the use of a transgenic mouse strain (FVB/TIE2-TK), where we will selectively ablate TEMs. Additionally, we will achieve TEMs depletion through the inhibition of a Tie2 ligand (i.e. Angiopoietin 2), through systemic administration of an anti Angiopoietin 2 antibody.

In summary, the project I am proposing is translational in nature and aims to confirm in human subjects findings obtained in a mouse model of corneal neovascularization. This will provide insight into the efficacy of potential treatments.

MATERIALS AND METHODS

Mice. Female FVB mice, purchased from Charles River Laboratories (Calco, Milan, Italy) and FVB/TIE2-TK transgenic mice, generated as previously described (De Palma et al, 2005), were used. Mice were anesthetized with intraperitoneal injection of Tribromoethanol (250 mg/kg) prior to any surgical procedure. All procedures were done according to protocols approved by the Animal Care and Use Committee of the San Raffaele Scientific Institute, in accordance with the ARVO Statement for the Use of Animals in Ophthalmic and Vision Research and the Italian Ministry of Health.

Corneal neovascularization models. Mice were anesthetized and CNV was induced by chemical burn or intrastromal suture placement as previously described (Ambati et al, 2006; Liu et al, 2011). Six or ten days later animals were euthanized and corneas removed. Corneal photographs were taken prior to the sacrifice with a biomicroscope using a digital camera (EOS 30D; Canon, Tokyo, Japan) attached to the slit-lamp microscope (Photoslitmap, model 40 SL-P; Zeiss, Oberkochen, Germany).

Corneal epithelium debridement model. Mice were anesthetized and corneas scraped with (i) a dulled blade to remove the corneal epithelium or (ii) a rotating burr (Algerbrush II, Janach, Como, Italy) to remove both epithelium and basement membrane, as described previously (Pal-Ghosh et al, 2011). After two or ten days, animals were sacrificed and eyes removed for immunohistochemical analysis.

TEM-depletion. Bone marrow transplantation**.** Six-week-old FVB or FVB/TIE2-TK transgenic mice were killed with CO_2, and their bone marrow (BM) was harvested by flushing the femurs and the tibias. 10^7 total BM cells were infused into the tail vein of lethally irradiated (975 cGy) 6- to 8-week-old FVB mice. The DNA extracted from the donor BM, together with the DNA extracted from the peripheral blood of each transplanted mouse 6-8 weeks after BM transplantation, were used to quantify the number of integrated LV copies/cell genome (vector copy number, VCN) by qPCR (Applied Biosystem) of vector sequences as previously described (De Palma et al, 2005).

GCV treatments. Eight weeks after bone marrow transplantation, TIE2-TK BMT and wild-type (WT) BMT mice were sutured and treated with *topical* Ganciclovir (GCV) (Virgan®, 1.5 mg/g) or phosphate buffered saline (PBS;

Sigma-Aldrich, St- Louis, MO) three times a day, for 10 days. Two independent experiments with a total of n=11-12 mice/group were performed.

Anti-ANG2 treatments. Starting at the moment of suture placement, 8-10-week-old mice received intra-peritoneal injections of 10 mg/kg of an anti-ANG2 antibody (Brown et al, 2010), control immunoglobulins (IgGs) or vehicle (PBS) every third day, for 10 days. Two independent experiments with a total of n=7-12 mice/group were performed.

In vivo EdU incorporation. Ten days after suture placement, 8-week-old mice (n=6) received two intra-peritoneal injection of a 1 mg/ml solution of Edu (Click-iT™ Imaging Kit; Invitrogen), 4 and 2 h prior to sacrifice.

Immunostaining and confocal microscopy on murine corneas. Whole mounts. Corneas were microsurgically excised under a stereomicroscope and immunostained according to our published protocol (Ferrari et al, 2013). Tissues were incubated overnight at 4°C with the following primary antibodies: goat anti-mouse MMR (MRC1) (1:200 dilution, AF2535; R&D Systems), rat anti-mouse CD11b-PE (1:100 dilution, 553311; BD Pharmigen), hamster anti-mouse CD11c-APC (1:100 dilution, 553802; BD Pharmigen), rat anti-mouse CD45-APC (1:400 dilution, 559864; BD Pharmigen), rat anti-

mouse TIE2-biotin (1:50 dilution, 13-5987-85; eBioscence), rat anti-mouse CD31 (1:200 dilution, 102501; BioLegend), rabbit anti-mouse LYVE1 (1:400 dilution, ab14917; AbCam), rat anti-mouse GR1-PE (1:50 dilution, 108408; BioLegend). For proliferation studies, cornea whole mounts were processed for detection of incorporated Edu and co-stained with anti-MRC1 antibody. Cryosections. On day 10, eyes were removed and fixed with paraformaldehyde (PFA) 4% (Sigma-Aldrich, St. Louis, MO) for 2 h at RT. After gradient dehydration in 10%, 20% and 30% sucrose in PBS each for 2 h, the samples were embedded in optimal cutting temperature (OCT) medium (Killik, Bio-Optica, Milan) and sectioned at 10 µm. Cryosections were stained as previously described(Ferrari et al, 2013). Antibodies used were rabbit anti-mouse ANG2 (1:200 dilution, ab8452; AbCam) and rat anti-mouse CD31. For the basement membrane immunostaining, 7 µm-thick cryosections were fixed with PFA 4% for 20 min, washed with PBS and blocked with 0.1M Glycin (Sigma-Aldrich) for 30 min at RT. After blocking, samples were incubated in 0.5% Trypsin (Cat. No 15400-054 Invitrogen/Gibco) for 15 min at 37°C, blocked with 10% cow serum and stained with goat anti-mouse Collagen IV (1340-01, 1:100 dilution; Southern Biotech).

Confocal microscopy (model TCS SP5; Leica Microsystems, Wetzlar, Germany) was used to capture all images with the exception of Fig. 3, panels:

3, 7 and 11 (corneal reconstruction), Fig. 7D and Fig. 8 which were taken by epifluorescent microscopy (model CTR5500. Leica Microsystems, Wetzlar, Germany). Confocal imaging was performed at 1 μm-slide thickness (10 μm z-stack) using x40 and x60 oil-immersion objective. Adobe Photoshop (Adobe Systems, Inc, CA, USA) was used for digital reconstruction of whole-mounted corneas by superimposition of overlapping images acquired at 5x or 10x magnification.

Immunostaining, confocal microscopy and immunohistochemistry in human samples. Avascular keratoconic and vascularized corneas removed during routine corneal transplant procedures were used. Whole-mounts. For immunostaining, the corneal stroma and epithelium were separated after 45-min incubation at 37°C in PBS containing 20 mM EDTA. After separation, corneal stromas were fixed for 30 min in ice-cold acetone, washed with PBS three times and blocked for 1 h at RT with 2% BSA. Tissues were incubated overnight at 4°C with rabbit anti-human Von Willebrand Factor (VWF) (1:400 dilution, A0082; Dako), mouse anti-human CD206-PE (MRC1) (1:100 dilution, 555954; BD Pharmingen) diluted in 2% BSA. The corneas were then washed and incubated for 2 h at RT with AlexaFluor 488 donkey anti-rabbit and AlexaFluor 594 donkey anti-mouse (1:500 dilution, A21203; Invitrogen) in 2% BSA. The whole-mounts were mounted using Vectashield

mounting medium with DAPI on glass slides and observed by confocal and epifluorescence microscopy as described above. Cryosections. Human corneas were fixed with PFA 4% overnight, dehydrated in 10%, 20%-30% sucrose in PBS each for 2 h and embedded in OCT. 10 µm-thick cryosections were blocked in 2% BSA and 0.3% Triton X-100 in PBS for 2 h at RT and stained with mouse anti-human CD206-PE (1:100 dilution, 555954; BD Pharmigen), CD45-APC (1:100 dilution, 130-091-230 Miltenyi Biotec) and mouse IgG1 isotype control (1:100 dilution, IC002P; R&D Systems). Paraffin embedded sections. For immunhistochemistry, 10% formalin fixed and paraffin embedded samples were incubated in unmasking solution (Tris pH 9) for 30 min at 97°C, incubated for 1 h at RT with mouse anti-human ANG2 (1:100 dilution, sc-74403; Santa Cruz Biotechnology), rinsed in PBS and detected with UltraVision Quanto Detection System HRP DAB (Thermo Scientific, CA, USA).

Statistical analysis. Data were analyzed by unpaired Student's t-test and differences between groups were considered statistically significant with $p<0.05$. All results are expressed as mean ± standard error of the mean (S.E.M.).

Flow cytometry. Four to six murine corneas were excised, pooled, and made into single cell suspensions by collagenase IV (0.2 mg/ml, Worthington), dispase (2 mg/ml, Gibco) and DNase I (0.1 mg/ml, Roche) treatment in IMDM medium supplemented with 5% fetal calf serum (FCS). After 30 min at 37°C in a shaking bath, cell suspensions were 40 μm-filtered and washed in cold PBS containing 2 mM EDTA and 0.5% BSA.

For flow cytometry, we used a BD FACSCanto (BD Bioscience) apparatus. All cell suspensions were incubated on ice with rat anti-mouse FcγIII/II receptor (CD16/CD32) blocking antibodies (4 μg/ml; BD Inc.) for 15 minutes on ice. They were then stained for 30 min at 4°C with the following primary antibodies: rat anti-mouse CD45-PB (1:100 dilution, 553081; BD Bioscience), rat anti-CD11b-APC-eFluor780 (1:300 dilution, 47-0112-82; eBiosciences), hamster anti-CD11c-APC (1:100 dilution, 550261; BD Bioscience) and rat anti-mouse MRC1-Biotinilated (1:50 dilution, C068C2; Biolegend). After antibody staining, the cells were washed, stained with streptavidin-PE (1:250 dilution, 554661; BD Bioscience) for 30 min at 4°C, washed and re-suspended in 7-amino-actinomycin D (7-AAD)-containing buffer, to exclude nonviable cells from further analyses.

We analyzed TEMs gated as $7AAD^{-}CD45^{+}CD11b^{+}MRC1^{+}CD11c^{-}$ cells (Fig. 5).

Quantification of cells and vessels. Eight to twelve whole-mounted corneas were examined for each staining. Nine different areas were examined in the periphery (in proximity to the suture) and three in the center of each cornea. The number of positive cells per field was counted using ImageJ software (ImageJ 1.44p; National Institutes of Health, Bethesda, MD). Cell counts were then averaged for the center and periphery of each cornea and used for statistical analysis. Quantitative analysis of vessels was performed using ImageJ software as previously described47. The area of the cornea covered by neovessels was outlined and the ratio between this value and the total area of the cornea was calculated (neovascular index) and used for statistical analysis.

Isotype control immunostaining. For the isotype controls the following isotype IgGs were used: rat IgG 2a,κ-PE (553930; BD Pharmigen), rat IgG 2b,κ-FITC (553988; BD Pharmigen), rabbit IgG (011-000-003; Jackson ImmunoResearch), goat IgG (AB-108-C; R&D Systems); hamster IgG 1λ1-APC (553956; BD Pharmigen).

Analysis of Cytokine Transcripts by Real-Time PCR. Eight pools of two 10 days-sutured and control corneas were collected for the Real-Time PCR analysis. Epithelium and stroma were separated after 10-min incubation at

37°C in PBS containing 20 mM EDTA and RNasin Plus RNase Inhibitor (n2611; Promega, Milan, Italy) and then homogenized with Ultra-Turrax (IKA, Wilmington, NC, USA). Total RNA extraction, DNAse treatment, reverse transcription and real-time PCR reaction were performed as previously described46. Taqman Gene Expression Assays (Applied Biosystems, Foster City, CA) for ANG2 (Mm00545822_m1), Tie2 (Mm00443243_m1), MRC1 (Mm00485148_m1), KDR (VEGFR2 Mm01222421_m1), CD45 (PTPRC, Mm01293577_m1), VWF (Mm00550376_m1), PROX1 (Mm00435969_m1) and GAPDH (Mm99999915_g1) were used. Results are presented as relative expression of 16 normal corneas pooled in pairs (ΔΔCT method).

RESULTS

In order to study CNV *in vivo*, we employed two different and extensively used murine models (Ambati et al, 2006; Liu et al, 2011): (i) placement of intrastromal sutures, which induces sectorial vessel growth, and (ii) cornea alkali burn, which results in extensive 360 degrees neovessel growth. A schematic representation of these models is presented in Fig. 1.

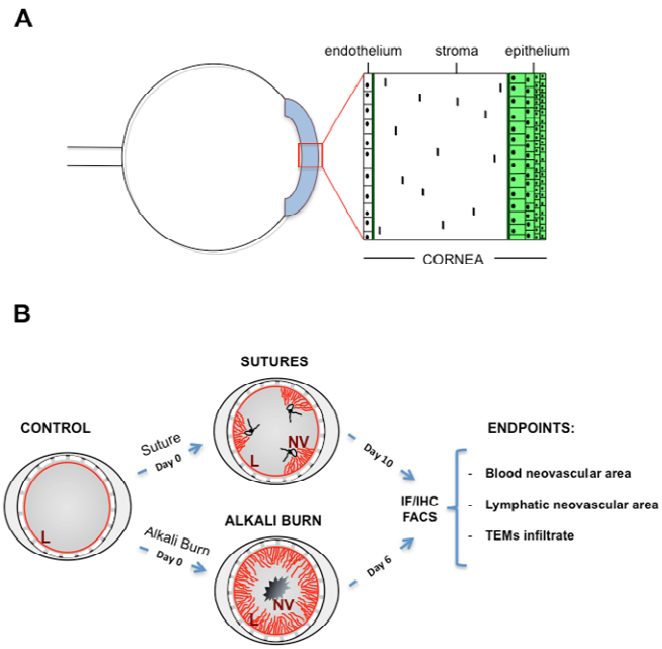

Figure 1. Schematic representation of the cornea and experimental design.

A Representation of the three layers of the cornea. From the outside to the inside of the cornea: epithelium, stroma and endothelium can be seen.

B Schematic representation of animal models of corneal neovascularization: control, sutured and alkali burned corneas. Endpoint readouts are also indicated. L = limbal arcade, NV = neovessels.

TEMs are present in the normal cornea and express MRC1 and LYVE1 markers

In order to test whether TEMs are associated with CNV, we performed confocal analysis on whole mount normal (avascular) and neo-vascularized mouse corneas. Unexpectedly, $TIE2^+$ cells were present in normal, avascular cornea. They were located in the corneal middle layer, namely the stroma. These cells also stained positive for the hematopoietic markers CD45 and CD11b, thus confirming their myeloid origin. Moreover, they expressed the scavenger receptor MRC1 and the hyaluronan receptor LYVE1, two markers of TEMs (Pucci et al, 2009). As expected, $TIE2^+$ cells were CD31 low and did not express CD11c (Pucci et al, 2009). In the quiescent cornea, all $CD45^+$ cells showed TEMs markers, with the exception of rare $CD11c^+$ cells. Intriguingly, TEMs were orderly arranged and homogeneously distributed throughout the corneal stroma (Fig. 2A-C, upper panels) and were absent in the corneal epithelium and endothelium (Fig. 7C). CNV was associated with a substantial increase in the number of $TIE2^+$ cells in the cornea without

changes in their marker profile ($MRC1^{+}CD11b^{+}CD11c^{-}$ $CD45^{+}LYVE1^{+}CD31^{low}$) (Fig. 2A-C, lower panels). After suture placement, we also observed infiltration of other bone marrow-derived cells (Fig. 2A lower panels, $CD45^{+}TIE2^{-}MRC1^{-}$), including $GR1^{+}$ granulocytes (Fig. 2D). However, upon injury, $GR1^{+}$ cells appeared mainly concentrated in the area of tissue damage (i.e. suture), while TEMs were homogeneously scattered around the entire cornea.

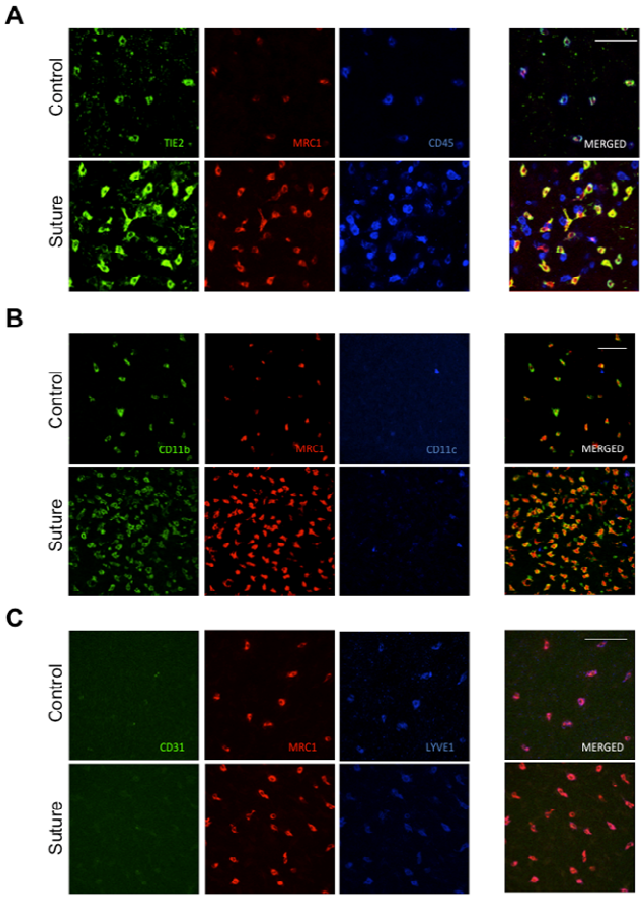

D

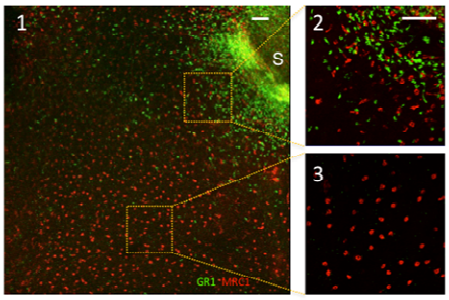

Figure 2. Corneal Tie2$^+$ cells are MRC1$^+$ myeloid cells residing in the stroma and increasing during neovascularization.

A-C Confocal immunofluorescence analysis on whole mounts of normal (upper panels) and 10 days sutured (lower panels) corneas. (A) Immunostaining for TIE2 (green), MRC1 (red) and CD45 (blue). All Tie2$^+$ cells express MRC1 and CD45. (B) Immunostaining for CD11b (green), MRC1 (red), CD11c (blue). All MRC1$^+$ cells are myeloid (CD11b$^+$) and do not express CD11c. (C) Immunostaining for CD31 (green), MRC1 (red) and LYVE1 (blue). MRC1$^+$ macrophages express LYVE1 and low levels of CD31. All isotype control stainings are shown in Fig. 3A. Scale bar = 100 µm.

D Confocal image for GR1$^+$ granulocytes (green) and MRC1$^+$ macrophages (red) 10 days after suture placement. Panel 1: low magnification of granulocyte and macrophage distribution in the cornea. Note that granulocytes mainly accumulate in the area of corneal injury (suture, S), while TEMs infiltrate the entire neovascularized cornea.

Panel 2, 3: representative images at higher magnification. Scale bar = 100µm.

Immunostaining with isotype control antibodies are provided below.

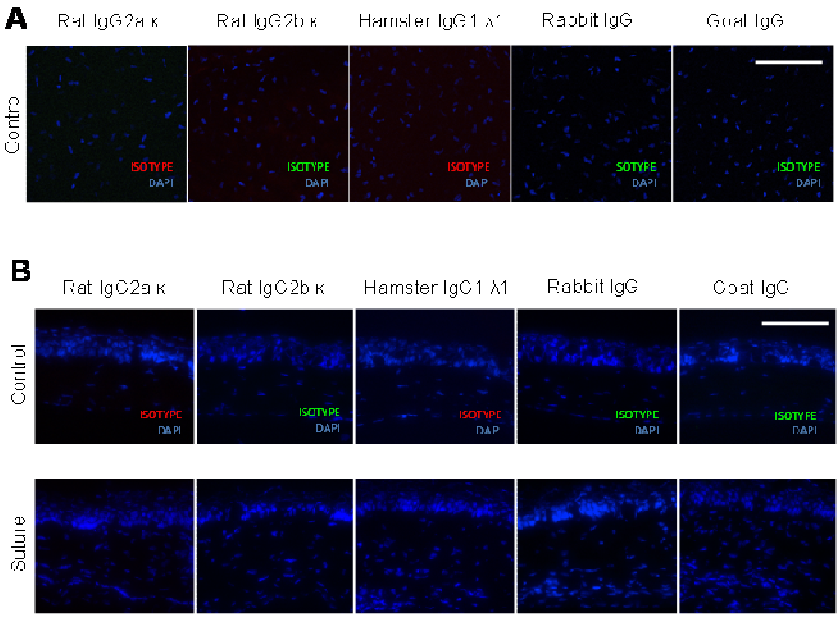

Fig. 3. Isotype controls. Isotype control immunostaining on whole mounts of quiescent corneas for all the antibodies used. Scale bar = 100 µm. Isotype control immunostaning on cryosections of normal and sutured corneas for all the antibodies used. Scale bar = 100 µm.

Quantification of MRC1^{+} cells on corneal whole mounts revealed no differences in cell density between the central and peripheral region of the avascular cornea (Fig. 4A and 4B), while a threefold increase was observed 10 days after suture in both regions of the injured cornea. The same fold increase was observed by flow cytometry 6 days upon alkali burn (Fig 4C). A sample for the gating strategy used is provided in Fig. 5

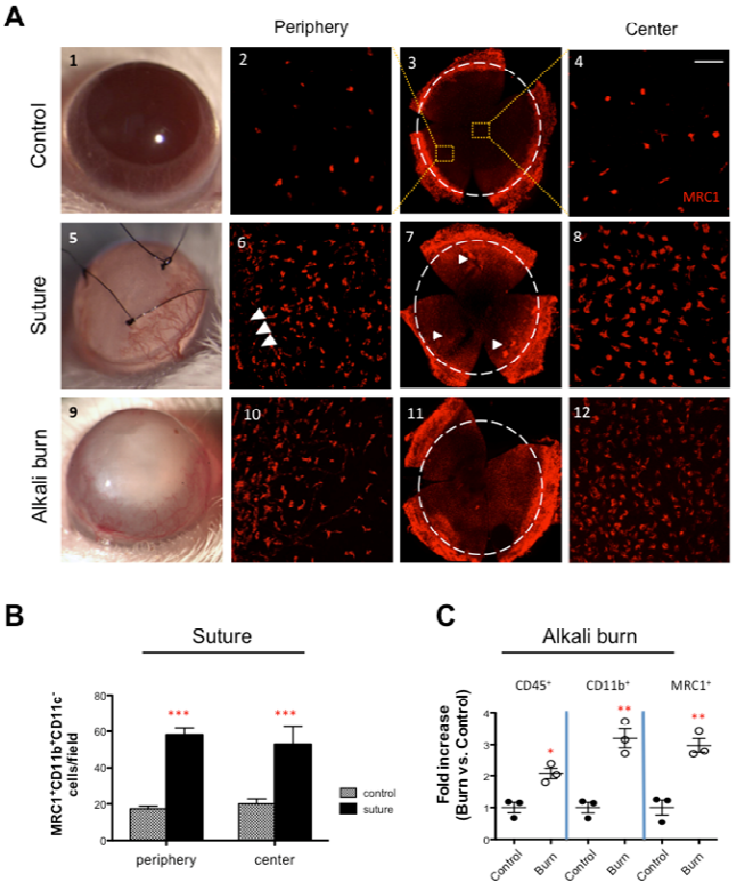

Figure 4. MRC1$^+$ macrophages are present in normal corneas and increased in two models of corneal neovascularization.

A Panels 1, 5, 9: representative slit-lamp pictures of control, sutured and alkali burned eyes. Panels 3, 7, 11: representative MRC1 (red) immunostaining of corneal whole-mounts 6 days (alkali burn) and 10 days (suture) upon induction of neovascularization. Arrowheads show suture placement. Dashed line shows the limbal arcade. Panels 2, 6, 10: representative high magnification images of MRC1 (red) immunostaining in the peripheral area of the cornea near the limbal arcade. Panels 4, 8, 12: representative high magnification images of MRC1 (red) immunostaining in the central cornea. Scale bar = 100μm.

B Quantitative confocal analysis of MRC1$^+$CD11b$^+$CD11c$^-$ cells in control (n=4 corneas) and sutured corneas (n=4 corneas) 10 days upon injury. Note the significant increase in both central and peripheral cornea.

C Flow cytometry analysis of MRC1$^+$ macrophages in quiescent (n=3 pools of 4 corneas) and causticated corneas (n=3 pools of 4 corneas) 6 days upon injury. Causticated corneas show significant increase in the percentage of hematopoietic CD45$^+$ cells, myeloid CD45$^+$CD11b$^+$ cells and MRC1$^+$CD11c$^-$ macrophages. Statistical analysis by unpaired Student's t test (* $p<0.05$, ** $p<0.01$, *** $p<0.001$).

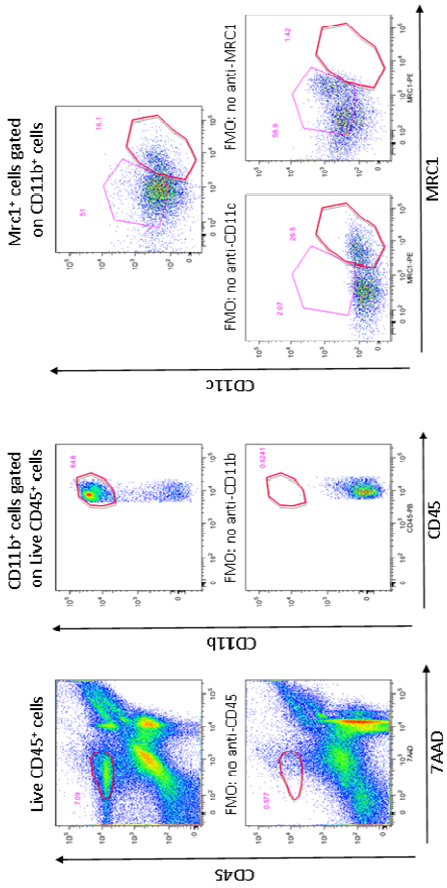

Fig. 5. Gating strategy used to detect hematopoietic cell populations in the cornea of quiescent and wounded corneas via FACS analysis. Cornea-derived cell suspensions (see online methods) were stained with 7-AAD to exclude non-viable cells from further analysis. Viable infiltrating hematopoietic cells were identified as 7-AAD^{-}CD45^{+} cells and, among them, myeloid cells (CD11b+) were further analyzed for their expression of CD11c and MRC1.

Fluorescence-minus-one (FMO) stained samples were used to gate marker-positive cells.

Real-Time PCR analysis on mRNAs extracted from 10 day sutured corneas confirmed a strong increase in the expression of several hematopoietic and endothelial cell markers in the stroma of sutured corneas (Fig. 6A) consistent with the observed increase in $CD45^{+}MRC1^{+}$ TEMs and the concurrent development of blood and lymphatic neovessels. No major changes were observed in the epithelium with the exception of a moderate increase in the levels of CD45 and MRC1 mRNAs (Fig. 6B).

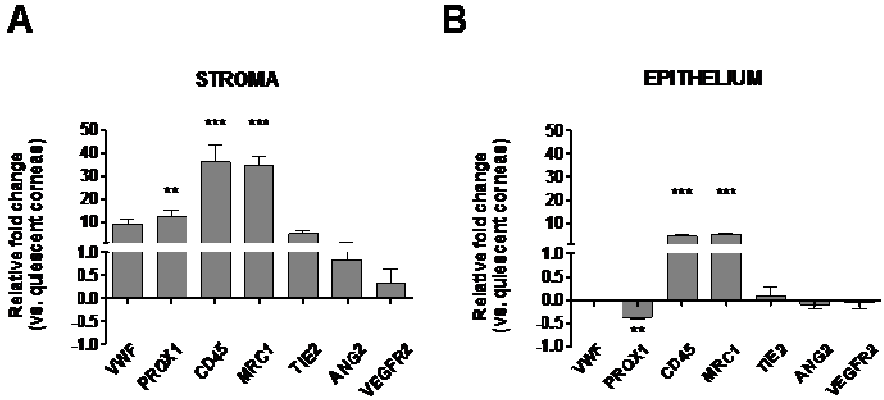

Fig. 6. Real-time PCR quantification of mRNA extracted from epithelium and stroma of control and sutured corneas at day 10. **(A-B)** Relative mRNA expression levels in the stroma and epithelium of sutured corneas (mean fold change over quiescent corneas ± S.E.M.; n = 8 corneas/group). Transcript

levels of CD45 and MRC1 were increased in the epithelium of sutured mice as opposed to control mice, while VWF, PROX1, CD45 and MRC1 mRNA were strongly increased in the stroma. Statistical analysis by unpaired Student's t test (** $p<0.01$, *** $p<0.001$).

TEMs localize adjacent to newly forming blood but not lymphatic vessels in the injured murine cornea

TEMs not only increased in number during corneal angiogenesis, but also showed peculiar morphologic modifications. TEMs found in the normal cornea or located far away from neovessels upon corneal injury were roundish in shape. However, TEMs found closer to the area of vascularization showed a ramified, spindle-like shape with several cell processes, suggesting active motility (Fig. 7A). Moreover, and especially at later stages post-injury, TEMs were also found in a characteristic peri-vascular location, "side-tracking" the course of the newly formed $CD31^{+}LYVE1^{-}$ blood vessels with constant spacing between TEMs and the underlying endothelial layer (Fig. 7B). Intriguingly, this vascular association was specific for blood vessels, as TEMs were found sparsely scattered around newly formed $CD31^{+}LYVE1^{+}$ lymphatic vessels (Fig. 7C). A 3D reconstruction of multiple confocal z-stack images of individual neovessels

confirmed the spatially organized perivascular distribution of TEMs around blood but not lymphatic vessels.

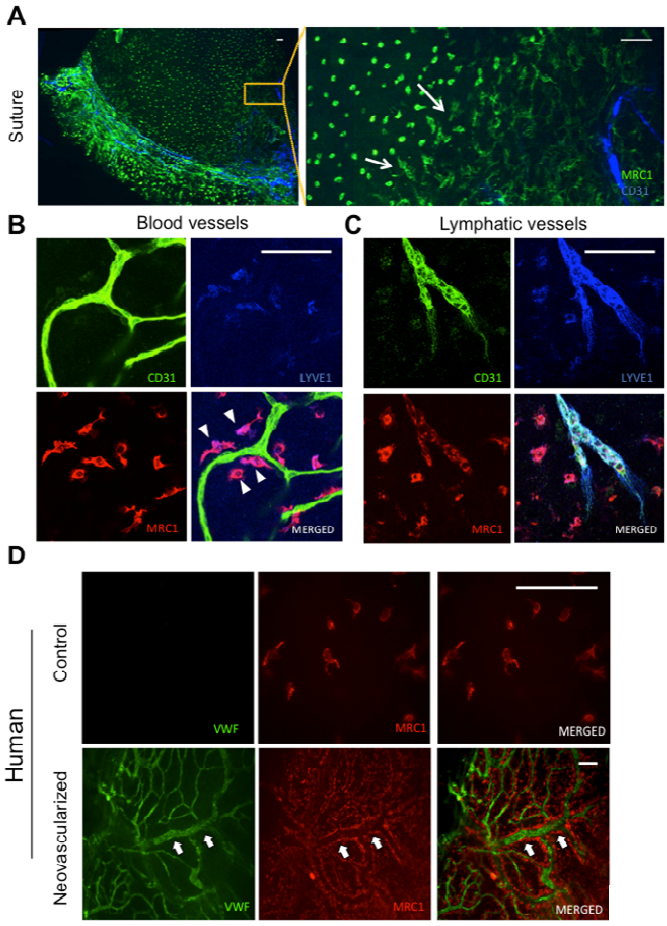

Figure 7. Human and murine MRC1$^+$ macrophages share a similar localization in quiescent and vascularized corneas.

A Murine MRC1$^+$ cells morphology. Confocal immunofluorescence of murine MRC1$^+$ macrophages (green) and CD31 vessels (blue) shows a progressive transition from spherical to spindle-shaped phenotype as they approach vessels in sutured corneas 10 days upon injury. Left

panel: partial confocal reconstruction of a whole mounted murine cornea. Right panel: high magnification showing morphological changes (arrows). Scale bar = 100µm.

B-C $MRC1^+$ cell localization in proximity of a (B) $CD31^+LYVE1^-$ blood neovessel and (C) $CD31^+LYVE1^+$ lymphatic neovessel. Note that $MRC1^+$ macrophages follow a "vessel track" distribution on blood (arrowheads) (B), but not on lymphatic vessels (C). Stainings: CD31 (green), LYVE1 (blue), and MRC1 (red). Scale bar = 100 □m.

D Representative epifluorescence images of vessels (VWF green) and $MRC1^+$ cells (red) in non-vascularized (keratoconus, upper panel) and neovascularized (lower panel) human corneas. Arrows show the association between $MRC1^+$ cells and vessels. Scale bar = 100µm.

$MRC1^+$ cells are present in the quiescent and neovascularized human cornea

Human avascular corneas (n=5) were obtained from patients affected by keratoconus and undergoing perforating keratoplasty. Immunofluorescence for the Von Willebrand Factor (VWF) confirmed that blood vessels were absent; however, scattered $MRC1^+$ cells were detected, thus suggesting that

MRC1$^+$ cells were present in avascular corneas (Fig. 7D upper panels), as we observed in murine corneas (Fig. 2C upper panels).

Human vascularized corneas (n=3) were also collected from patients undergoing perforating keratoplasty due to vascularized leucomas. Immunofluorescence revealed

extensive blood neovessels, which were almost completely wrapped by adjacent MRC1$^+$ cells (Fig. 7D lower panels). These MRC1$^+$ cells were also CD45$^+$, hence confirming their hematopoietic origin (Fig. 8A), similarly to what we observed in mice (Fig. 2A). Immunostainings with isotype control antibodies are provided in the supplementary materials (Fig. 8B).

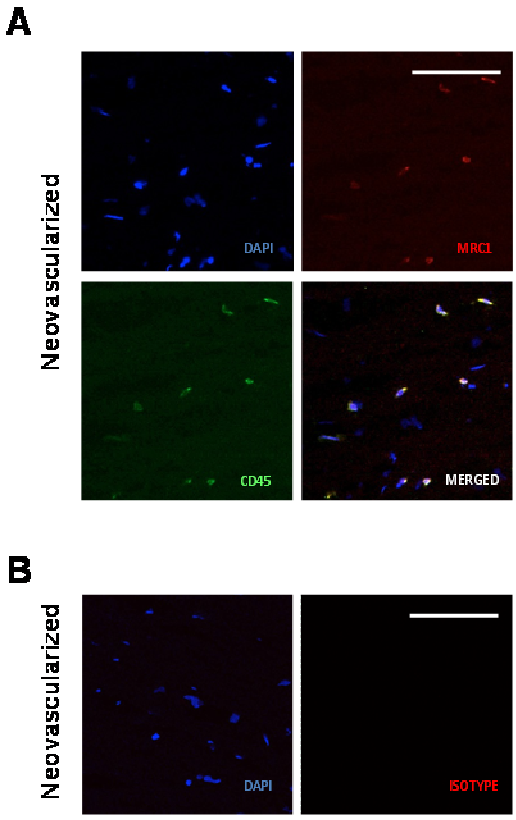

Fig. 8. **(A)** Immunostaining for CD45 (green) and MRC1 (red) macrophages on neovascularized human cornea cross sections. All $MRC1^+$ cells expressed the CD45 marker confirming their hematopoietic origin. **(B)** Control staining for CD45 and MRC1 using isotype-matched non specific antibody. Scale bar = 100 μm.

Overall, these data show that a population of macrophages with markers, anatomical distribution and response to injury similar to those described for TEMs in the mouse cornea is also found in the human cornea. These cells increase in number upon CNV, where they are consistently found adjacent to blood neo-vessels.

Specific TEMs depletion is associated with reduced corneal blood and lymphatic neovascularization

In order to test the functional requirement of TEMs in CNV, we transplanted mice with hematopoietic stem cells (HSC) from transgenic mice expressing a conditional suicide TK transgene under the control of the *Tie2* promoter, a model previously shown to allow selective depletion of TEMs following Ganciclovir (GCV) administration (De Palma et al, 2005). We then induced CNV by means of corneal sutures and administered GCV *topically* to the cornea three times a day for 10 days.

We observed a significant reduction ($p<0.01$) of corneal $MRC1^+$ cell number in the TK+GCV group when compared with the control groups TK+PBS (32% reduction) and wild type+GCV (41% reduction), (Fig. 9A). These data indicate that, after HSC transplantation and corneal injury, a substantial fraction of TEMs found in the cornea are of donor origin (i.e. they express the TK transgene) and undergo *in situ* proliferation, where they become exposed to the killing action of GCV. Indeed, when mice were euthanized shortly after an *in vivo* EdU pulse to label cycling cells, we observed labeled TEMs in corneas undergoing neovascularization while none was marked in normal corneas (1.18±0.28 cells/field in vascularized corneas vs. 0 cells in normal corneas; $p<0.001$) (Fig. 9D). We cannot discriminate, however, whether the *in situ* proliferating cells were recruited acutely post-injury from the circulation, or originated from the resident pool. Interestingly, both blood (Fig. 9B) and lymphatic (Fig. 9C) neovessels were significantly reduced in CNV upon TEMs depletion, as shown by measuring the vessel invasion area (blood invasion area: 0.48±0.05 TK+GCV vs. 0.58±0.07 TK+PBS, $p<0.01$ and 0.57±0.10 wild-type+GCV, $p<0.05$; lymphatic invasion area: 0.3±0.05 TK+GCV vs. 0.43±0.14 TK+PBS and 0.39±0.13 wild-type+GCV; $p<0.01$). These data indicate a pro-angiogenic role of $MRC1^+$ TEMs during CNV.

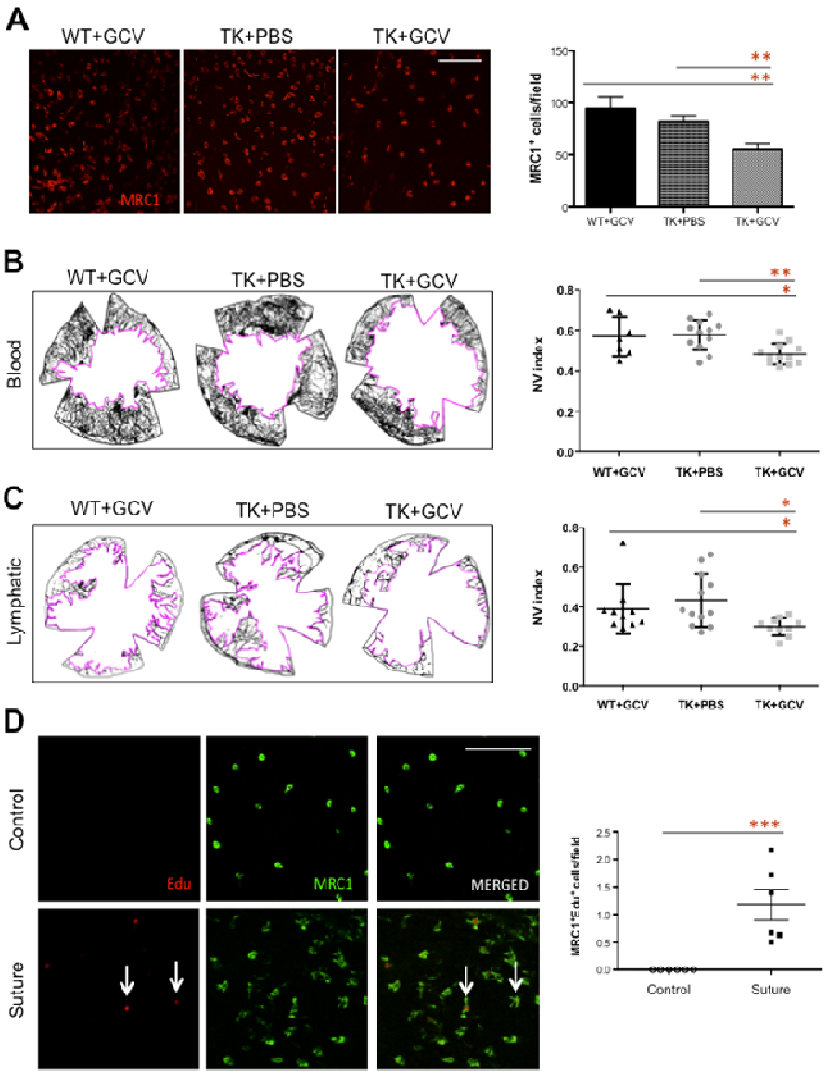

Figure 9. Selective depletion of Tie2^{+}MRC1^{+} macrophages inhibits blood and lymphatic neovessel formation in sutured corneas.

A-C MRC1^{+} cells and corneal neovascularization 10 days after suture placement in mice transplanted with total bone marrow from TIE2-TK

(TK) or wild-type (WT) donor mice and treated with topical ganciclovir (GCV) or PBS. (A) Representative confocal images of $MRC1^+$ cells in control (WT+GCV and TK+PBS) and depleted (TK+GCV) corneas. The histogram on the right shows a significant reduction in the number of $MRC1^+$ cells in the sutured corneas upon depletion of $Tie2^+$ macrophages (mean value ± S.E.M.; n=7-12 corneas/group, in each cornea 9 peripheral images were quantified). (B, C) Representative images of $CD31^+$ blood neovessel and $LYVE1^+$ lymphatic neovessel in control (WT+GCV and TK+PBS) and depleted (TK+GCV) corneas. Scatter plots at right show significant reduction in the vascularized area of both blood and lymphatic neovessels (NV index; mean value ± S.E.M.; n=7-12 corneas). Data from one of two independent experiments are presented.

D Representative confocal images (left) and quantitative analysis (right) of proliferating $MRC1^+$ macrophages (Edu^+MRC1^+ cells) in quiescent and sutured corneas 10 days upon injury and 4 h upon first Edu injection. No proliferating cells were observed in the control corneas but a few Edu^+MRC1^+ cells are observed 10 days after suture placement (white arrows). Stainings: Edu (red), MRC1 (green). Statistical analysis by unpaired Student's t test (* $p<0.05$, ** $p<0.01$, *** $p<0.001$); (n=6

corneas, in each cornea 9 peripheral images were quantified). Scale bar = 100 μm.

Mouse and human quiescent corneas contain Angiopoietin 2 and its anatomical localization is changed during CNV

To investigate the contribution of the Tie2/ANG2 pathway in CNV, we analyzed ANG2 expression in the normal and vascularized cornea by immunostaining and Real-Time PCR. Surprisingly, ANG2 was constitutively and highly expressed in the normal, avascular cornea of both human subjects and mice as shown by immunohistochemistry and immunofluorescence (Fig. 10A, panels 2 and 5). The highest expression was in the epithelium, where it showed a dotted cytoplasmic localization mostly found around the epithelial cell nuclei. Lower levels of expression were also detectable in endothelial cells of both humans and mice. The quiescent stroma, starting immediately underneath the epithelial basal membrane, did not stain for ANG2. Neovascularized corneas, however, showed increased scattered ANG2 staining throughout the stroma, partially associated with the neovessels (Fig. 10A, panels 3 and 6). Isotype control immunostainings are shown in Fig. 10A, panels 1,4 and Fig. 3B. Importantly, Real-Time PCR showed no increase in the levels of *ANG2* mRNA after injury (Fig. 6A and B), thus suggesting a possible relocation of ANG2 from the injured epithelium into the stroma.

Angiopoietin 2 inhibition results in reduced blood and lymphatic neovascularization

Finally, we treated mice undergoing CNV with a monoclonal antibody specifically reacting against human and mouse ANG2 (3.19.3, AstraZeneca, Delaware, USA) (Brown et al, 2010). The anti-ANG2 antibody was administered intraperitoneally and compared with control IgG or PBS treatment. ANG2 blockade significantly reduced the number of corneal TEMs when compared with control PBS (37.6% reduction, $p<0.05$) or IgG (38.9% reduction, $p<0.001$) (Fig. 10B). Even more interestingly, both blood and lymphatic neovessels were significantly reduced ($p<0.001$), (Fig. 10C and D). These results suggest that pharmacological ANG2 blockade may represent a promising therapeutic approach to inhibit CNV.

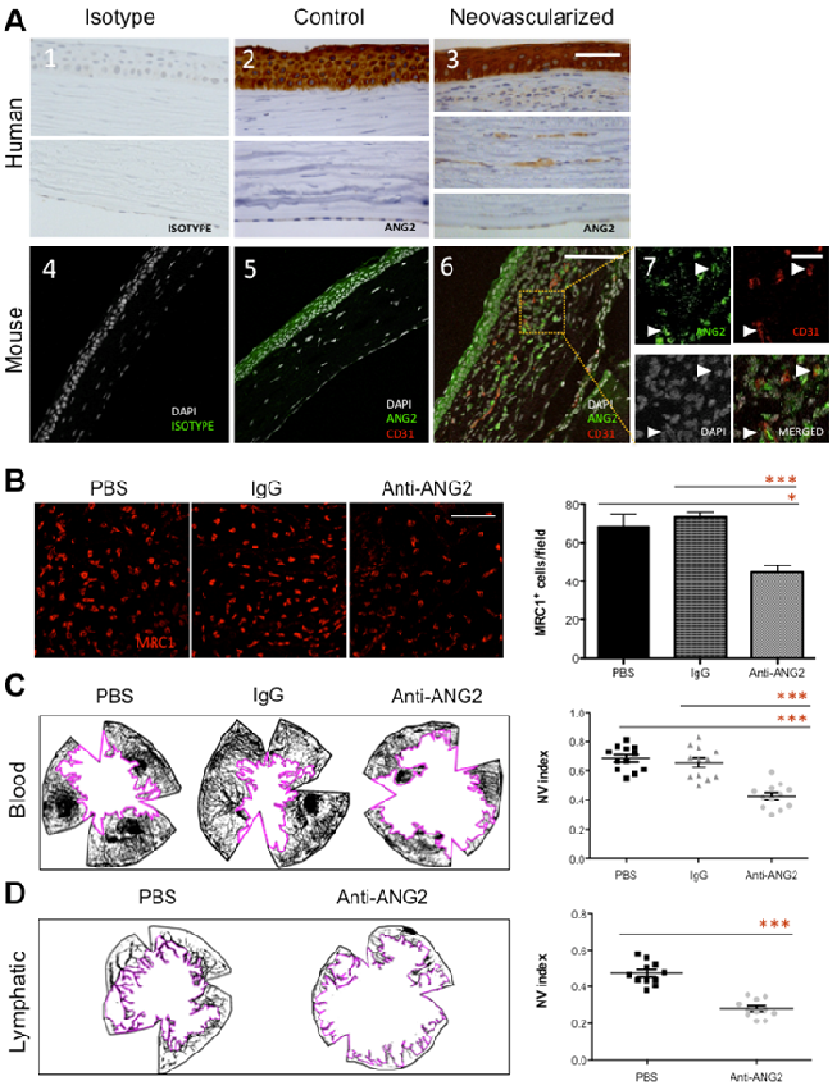

Figure 10. Angiopoietin 2 is required for corneal neovascularization and is expressed in both human and murine quiescent corneas.

A Expression and localization of ANG2 in normal and neovascularized human and murine corneas. Panel 1-3: immunohistochemistry for ANG2 in control and neovascularized human corneas. Panel 4-7:

immunofluorescence staining for ANG2 (green) and CD31 (red) in control and neovascularized murine corneas (scale bar = 100 μm). A higher magnification of a stromal area from panel 6 is presented in panel 7 (scale bar = 50 μm). Note that ANG2 colocalizes with $CD31^+$ neovessels. Control staining for ANG2 using isotype-matched non specific antibodies is provided in panels 1 and 4.

B-D *In vivo* pharmacological blockade of ANG2. Treatment was started at the time of suture placement and continued for 10 days. (B) Representative confocal images (left) and quantitative analysis of $MRC1^+$ cells (right) showing a significant reduction in the treated group (mean value ± S.E.M.; n = 12 corneas/group, in each cornea 9 peripheral images were quantified). (C, D) Representative images of $CD31^+$ blood neovessel (C) and $LYVE1^+$ lymphatic neovessel (D) in control (PBS and IgG) and treated (anti-ANG2) corneas. Scatter plots at right show significant reduction in the vascularized area of both blood and lymphatic neovessels (NV index, n=12 corneas/group). Data from one of two independent experiments are presented. Scale bar = 100 μm. Statistical analysis by unpaired Student's t test (* $p< 0.05$, *** $p<0.001$).

Epithelial basal (Bowman) membrane disruption results in increased Angiopoietin 2 diffusion into the stroma

High levels of ANG2 stored in the corneal epithelium might represent a reservoir physically separated from the stroma by the Bowman (basal) membrane, as it is the case for TGFβ2 (Stramer et al, 2003). This reservoir, however, could be made immediately available to the stroma upon epithelial injury and disruption of the Bowman membrane. To test whether the Bowman membrane may help in sequestering ANG2 released from the epithelium, we compared two different corneal debridement models: the dulled blade and rotating burr wounding models (Pal-Ghosh et al, 2011) (Fig. 11A), the first retaining and the second interrupting the Bowman membrane integrity. Bowman membrane removal in the rotating burr, but not in the dulled blade model was confirmed by collagen IV immunostaining as shown in Fig. 11B. Both types of injuries resulted in the progressive increase of stromal ANG2, however, the increase observed in the rotating burr model was two-fold higher than the one observed in the dulled blade model (10.80±1.51% total pixel in rotating burr wounds vs. 5.54±0.42% in dulled blade wounds; $p<0.001$), (Fig. 11C and D left-panel). Two days after wounding new vessels have not yet developed, thus excluding the contribution of vessel-derived ANG2, and suggesting that diffusion from the corneal epithelium was strongly enhanced by the interruption of the Bowman

membrane. Moreover, in the rotating burr model, the enhanced diffusion of ANG2 was associated with a three-fold increase in the number of $MRC1^+$ cell (36.58±2.12 cells/field in rotating burr wounds vs. 13.61±1.02 in dulled blade wounds; $p<0.01$), (Fig. 11C and D right-panel, day 10), neovessel density increased.

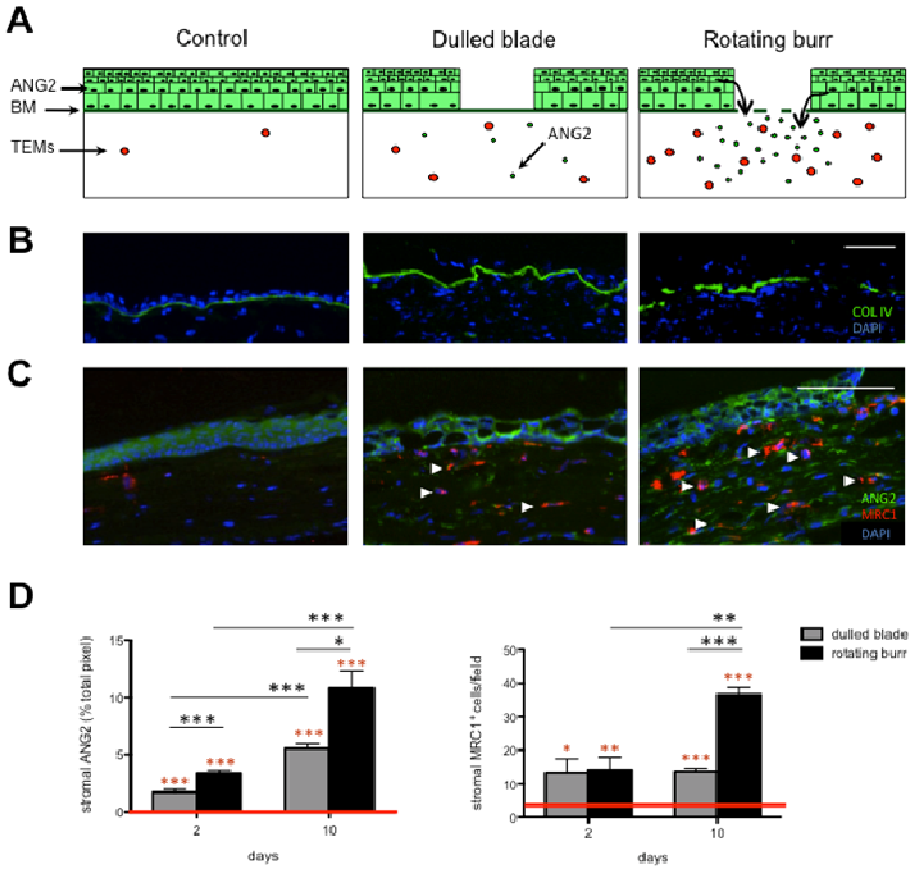

Figure 11. Interruption of the basal (Bowman) epithelial membrane results in increased ANG2 diffusion into the stroma.

A Schematic representation of the epithelial debridement models: control, dulled blade and rotating burr wounds. BM = Bowman Membrane.

B Immunostaining for collagen IV^+ Bowman membrane (green) in normal and wounded corneas. The basement membrane was interrupted in the rotating burr but not in the dulled blade wounds.

C Representative images of ANG2 (green) and $MRC1^+$ (red) immunostaining.

D Quantitative analysis of ANG2 levels and $MRC1^+$ cells in normal and wounded corneas (mean value ± S.E.M.; n = 6 corneas/group, in each cornea 27 sections were quantified). The red line represents the control group. Statistical analysis by unpaired Student's t test (* $p< 0.05$, ** $p<0.01$, *** $p<0.001$).

These data suggest that the Bowman membrane may indeed represent a physical barrier blocking ANG2 diffusion into the stroma and that its disruption is associated with a more rapid and significant increase in stromal ANG2. Immunostainings with isotype control antibodies are provided in Fig. 3.

DISCUSSION

We report that MRC1$^+$ TEMs, a specific subpopulation of pro-angiogenic macrophages, reside in the *avascular* corneal stroma in mice and humans. This was unexpected and never reported before. Interestingly, their number increases during CNV. Similarly, ANG2 is highly expressed in the normal corneal epithelium and increased during CNV. Selective blockade of TEMs proliferation or ANG2 was able to significantly reduce CNV. Also surprising was our finding that ANG2 is highly and exclusively expressed in the epithelium of avascular corneas, with an intracellular pattern highly reminiscent of sVEGFR-1. Indeed, a prior report found that the corneal epithelium constitutively expresses sVEGFR-1, which inhibits stromal angiogenesis (Ambati et al, 2006).

Our discovery in the corneal stroma of a pre-assembled and orderly network of TEMs, which are essential drivers for angiogenesis in other sites (De Palma et al, 2005; Fantin et al, 2010), may represent an evolutionary benefit in case of injury, as prompt, TEMs-mediated neovascularization could keep infections at bay and reduce the risks of corneal perforation.

It has been reported that ANG2 is involved in CNV (Yuen et al, 2014), although its expression in the avascular, human cornea and its complex relationship with TEMs were not investigated previously. Specifically,

ANG2 may elicit (Coffelt et al, 2010; Mazzieri et al, 2011; Venneri et al, 2007) or inhibit (Lobov et al, 2002) angiogenesis depending on the expression of other inflammatory mediators, such as VEGF (Holash et al, 1999), potentially allowing optimal tuning of neovascularization. In the cornea, this is of paramount importance as unnecessary neovascularization significantly impairs visual acuity.

Our study supports the existence of a novel mechanism regulating the growth of neovessels depending on the severity of the injury. We show that interruption of the basal Bowman epithelial membrane increases (doubles) ANG2 penetration in the stroma. As a consequence, stromal bound ANG2 can activate resident macrophages and induce CNV.

Further, we show that the presence of ANG2 in the epithelium and of $MRC1^+$ macrophages in the stroma is conserved in *human* quiescent corneas and increased upon neovascularization. It is worth noting that a critical role for macrophages in corneal angiogenesis was previously shown in relation to VEGF (Cursiefen et al, 2004), but not ANG2.

Finally, systemic administration of a monoclonal antibody targeting ANG2 (Brown et al, 2010) significantly attenuated neovascularization *and* TEMs infiltration. Interestingly, anti-ANG2 treatment also inhibited lymphangiogenesis, which has a key role in many systemic pathological conditions, such as tumor metastasis and transplant rejection, affecting

millions of people worldwide (Stacker et al, 2002; Yamagami & Dana, 2001). In these regards, combined anti-ANG2/anti-VEGF treatment may reduce CNV to a much greater extent than single agents do (Hashizume et al, 2010).

In summary, we propose that our results may have implications beyond the cornea, in the many processes where the control of angiogenesis could be beneficial, such as wound healing, atherosclerosis or stroke.

REFERENCES

Akpek EK, Dart JK, Watson S, Christen W, Dursun D, Yoo S, O'Brien TP, Schein OD, Gottsch JD (2004). A randomized trial of topical cyclosporin 0.05% in topical steroid-resistant atopic keratoconjunctivitis. Ophthalmology 111(3):476-82.

Albuquerque RJ, Hayashi T, Cho WG, Kleinman ME, Dridi S, Takeda A, Baffi JZ, Yamada K, Kaneko H, Green MG et al (2009) Alternatively spliced vascular endothelial growth factor receptor-2 is an essential endogenous inhibitor of lymphatic vessel growth. Nat Med 15**:** 1023-1030

Ambati BK, Nozaki M, Singh N, Takeda A, Jani PD, Suthar T, Albuquerque RJ, Richter E, Sakurai E, Newcomb MT et al (2006) Corneal avascularity is due to soluble VEGF receptor-1. Nature 443**:** 993-997

Augustin HG, Koh GY, Thurston G, Alitalo K (2009) Control of vascular morphogenesis and homeostasis through the angiopoietin-Tie system. Nature reviews Molecular cell biology 10**:** 165-177

Azar DT (2006) Corneal angiogenic privilege: angiogenic and antiangiogenic factors in corneal avascularity, vasculogenesis, and wound healing (an

American Ophthalmological Society thesis). Transactions of the American Ophthalmological Society 104**:** 264-302

Brown JL, Cao ZA, Pinzon-Ortiz M, Kendrew J, Reimer C, Wen S, Zhou JQ, Tabrizi M, Emery S, McDermott B et al (2010) A human monoclonal anti-ANG2 antibody leads to broad antitumor activity in combination with VEGF inhibitors and chemotherapy agents in preclinical models. Molecular cancer therapeutics 9**:** 145-156

Cao Y, Arbiser J, D'Amato RJ, D'Amore PA, Ingber DE, Kerbel R, Klagsbrun M, Lim S, Moses MA, Zetter B et al (2011) Forty-year journey of angiogenesis translational research. Science translational medicine 3**:** 114rv113

Chang JH, Gabison EE, Kato T, Azar DT (2001) Corneal neovascularization. Current opinion in ophthalmology 12**:** 242-249

Chang L, Kaipainen A, Folkman (2002) Lymphangiogenesis new mechanisms. J. Ann N Y Acad Sci.;979:111-9.

Chung ES, Saban DR, Chauhan SK, Dana R. (2009) Regulation of blood vessel versus lymphatic vessel growth in the cornea. Invest Ophthalmol Vis Sci.;50(4):1613-8.

Coffelt SB, Tal AO, Scholz A, De Palma M, Patel S, Urbich C, Biswas SK, Murdoch C, Plate KH, Reiss Y et al (2010) Angiopoietin-2 regulates gene expression in TIE2-expressing monocytes and augments their inherent proangiogenic functions. Cancer Res 70**:** 5270-5280

Cursiefen C, Chen L, Borges LP, Jackson D, Cao J, Radziejewski C, D'Amore PA, Dana MR, Wiegand SJ, Streilein JW (2004) VEGF-A stimulates lymphangiogenesis and hemangiogenesis in inflammatory neovascularization via macrophage recruitment. J Clin Invest 113**:** 1040-1050

Cursiefen C, Chen L, Saint-Geniez M, Hamrah P, Jin Y, Rashid S, Pytowski B, Persaud K, Wu Y, Streilein JW et al (2006) Nonvascular VEGF receptor 3 expression by corneal epithelium maintains avascularity and vision. Proceedings of the National Academy of Sciences of the United States of America 103**:** 11405-11410

Cursiefen C, Kruse F (2006). new aspects of angiogenesis in the cornea. Essential Ophthalmol, 83-99.

De Palma M, Mazzieri R, Politi LS, Pucci F, Zonari E, Sitia G, Mazzoleni S, Moi D, Venneri MA, Indraccolo S et al (2008) Tumor-targeted interferon-alpha delivery by Tie2-expressing monocytes inhibits tumor growth and metastasis. Cancer Cell 14**:** 299-311

De Palma M, Venneri MA, Galli R, Sergi Sergi L, Politi LS, Sampaolesi M, Naldini L (2005) Tie2 identifies a hematopoietic lineage of proangiogenic monocytes required for tumor vessel formation and a mesenchymal population of pericyte progenitors. Cancer Cell 8**:** 211-226

De Palma M, Venneri MA, Roca C, Naldini L (2003) Targeting exogenous genes to tumor angiogenesis by transplantation of genetically modified hematopoietic stem cells. Nat Med 9**:** 789-795

Fantin A, Vieira JM, Gestri G, Denti L, Schwarz Q, Prykhozhij S, Peri F, Wilson SW, Ruhrberg C (2010) Tissue macrophages act as cellular chaperones for vascular anastomosis downstream of VEGF-mediated endothelial tip cell induction. Blood 116**:** 829-840

Ferrari G, Bignami F, Giacomini C, Franchini S, Rama P (2013) Safety and efficacy of topical infliximab in a mouse model of ocular surface scarring. Invest Ophthalmol Vis Sci 54**:** 1680-1688

Gerten G. (2008) Bevacizumab (avastin) and argon laser to treat neovascularization in corneal transplant surgery. Cornea 27(10):1195-9

Gimbrone MA, Jr., Cotran RS, Leapman SB, Folkman J (1974) Tumor growth and neovascularization: an experimental model using the rabbit cornea. Journal of the National Cancer Institute 52**:** 413-427

Hanahan D, Folkman J (1996) Patterns and emerging mechanisms of the angiogenic switch during tumorigenesis. Cell 86**:** 353-364

Hashizume H, Falcon BL, Kuroda T, Baluk P, Coxon A, Yu D, Bready JV, Oliner JD, McDonald DM (2010) Complementary actions of inhibitors of angiopoietin-2 and VEGF on tumor angiogenesis and growth. Cancer Res 70**:** 2213-2223

Holash J, Maisonpierre PC, Compton D, Boland P, Alexander CR, Zagzag D, Yancopoulos GD, Wiegand SJ (1999) Vessel cooption, regression, and

growth in tumors mediated by angiopoietins and VEGF. Science 284**:** 1994-1998

Liu X, Lin Z, Zhou T, Zong R, He H, Liu Z, Ma JX, Liu Z, Zhou Y (2011) Anti-angiogenic and anti-inflammatory effects of SERPINA3K on corneal injury. PLoS One 6**:** e16712

Lobov IB, Brooks PC, Lang RA (2002) Angiopoietin-2 displays VEGF-dependent modulation of capillary structure and endothelial cell survival in vivo. Proceedings of the National Academy of Sciences of the United States of America 99**:** 11205-11210

Mantovani A, Sica A (2010) Macrophages, innate immunity and cancer: balance, tolerance, and diversity. Current opinion in immunology 22**:** 231-237

Mazzieri R, Pucci F, Moi D, Zonari E, Ranghetti A, Berti A, Politi LS, Gentner B, Brown JL, Naldini L et al (2011) Targeting the ANG2/TIE2 axis inhibits tumor growth and metastasis by impairing angiogenesis and disabling rebounds of proangiogenic myeloid cells. Cancer Cell 19**:** 512-526

Nucera S, Biziato D, De Palma M (2011) The interplay between macrophages and angiogenesis in development, tissue injury and regeneration. The International journal of developmental biology 55**:** 495-503

Ogawa S, Yoshida S, Ono M, Onoue H, Ito Y, Ishibashi T, Inomata H, Kuwano M (1999) Induction of macrophage inflammatory protein-1alpha and vascular endothelial growth factor during inflammatory neovascularization in the mouse cornea. Angiogenesis 3**:** 327-334

Pal-Ghosh S, Pajoohesh-Ganji A, Tadvalkar G, Stepp MA (2011) Removal of the basement membrane enhances corneal wound healing. Exp Eye Res 93**:** 927-936

Pillai CT, Dua HS, Hossain P (2000). Fine needle diathermy occlusion of corneal vessels. Invest Ophthalmol Vis Sci;41(8):2148-53.

Pucci F, Venneri MA, Biziato D, Nonis A, Moi D, Sica A, Di Serio C, Naldini L, De Palma M (2009) A distinguishing gene signature shared by tumor-infiltrating Tie2-expressing monocytes, blood "resident" monocytes,

and embryonic macrophages suggests common functions and developmental relationships. Blood 114**:** 901-914

Saharinen P, Bry M, Alitalo K (2010) How do angiopoietins Tie in with vascular endothelial growth factors? Current opinion in hematology 17**:** 198-205

Saharinen P, Eklund L, Pulkki K, Bono P, Alitalo K (2011) VEGF and angiopoietin signaling in tumor angiogenesis and metastasis. Trends in molecular medicine 17**:** 347-362

Sekiyama E, Nakamura T, Cooper LJ, Kawasaki S, Hamuro J, Fullwood NJ, Kinoshita S (2006) Unique distribution of thrombospondin-1 in human ocular surface epithelium. Invest Ophthalmol Vis Sci 47**:** 1352-1358

Singh N, Tiem M, Watkins R, Cho YK, Wang Y, Olsen T, Uehara H, Mamalis C, Luo L, Oakey Z et al (2013) Soluble vascular endothelial growth factor receptor 3 is essential for corneal alymphaticity. Blood 121**:** 4242-4249

Skobe M, Dana R (2009) Blocking the path of lymphatic vessels. Nat Med 15**:** 993-994

Stacker SA, Achen MG, Jussila L, Baldwin ME, Alitalo K (2002) Lymphangiogenesis and cancer metastasis. Nature reviews Cancer 2**:** 573-583

Stramer BM, Zieske JD, Jung JC, Austin JS, Fini ME (2003) Molecular mechanisms controlling the fibrotic repair phenotype in cornea: implications for surgical outcomes. Invest Ophthalmol Vis Sci 44**:** 4237-4246

Sugisaki K, Usui T, Nishiyama N, Jang WD, Yanagi Y, Yamagami S, Amano S, Kataoka K. (2008). Photodynamic therapy for corneal neovascularization using polymeric micelles encapsulating dendrimer porphyrins. Invest Ophthalmol Vis Sci. 49(3):894-9.

Titiyal JS, Negi S, Anand A, Tandon R, Sharma N, Vajpayee RB (2006) Risk factors for perforation in microbial corneal ulcers in north India. The British journal of ophthalmology 90**:** 686-689

Venneri MA, De Palma M, Ponzoni M, Pucci F, Scielzo C, Zonari E, Mazzieri R, Doglioni C, Naldini L (2007) Identification of proangiogenic

TIE2-expressing monocytes (TEMs) in human peripheral blood and cancer. Blood 109**:** 5276-5285

John P. Whitcher, M. Srinivasan and Madan P. Upadhyay Corneal blindness : a global perspective (2001). Bulletin of the World Health Organization : the International Journal of Public Health 2001 ; 79(3) : 214-221

Yamagami S, Dana MR (2001) The critical role of lymph nodes in corneal alloimmunization and graft rejection. Invest Ophthalmol Vis Sci 42**:** 1293-1298

Yuen D, Grimaldo S, Sessa R, Ecoiffier T, Truong T, Huang E, Bernas M, Daley S, Witte M, Chen L (2014) Role of angiopoietin-2 in corneal lymphangiogenesis. Invest Ophthalmol Vis Sci 55**:** 3320-3327